2015 IEEE International Conference on Advanced Intelligent Mechatronics (AIM)
July 7-11, 2015. Busan, Korea

A synthetic framework for evaluating the anthropomorphic characteristics of prosthetic hands

Yuan Liu*, Dapeng Yang, Member, IEEE , Li Jiang and Hong Liu

Abstract—**In order to improve the prosthetic hand's design and usability, this paper presents a synthetic framework for evaluating the current prosthetic hands' anthropomorphic features with 12 quantified prosthetic hand anthropomorphism evaluation indexes (QPHAEIs). Our primary results show that a global anthropomorphic score (GAS) of the current commercial prosthetic hands is only 45.2%. The compliance, coupling speed ratio and configuration of the degrees of freedom (DOF) are found to be the lowest three anthropomorphism evaluation indexes in all QPHAEIs. Besides these significant findings, a consideration priority order in prosthetic hand's anthropomorphic index design is also proposed. Further correlation analysis indicates that evaluation methods using rotation axis distribution, rather than experimental grasp gesture, are more reliable to measure a prosthetic hand's GAS.**

I. INTRODUCTION

After several decades' intensive studies on advanced prosthetic hands, an eligible robotic substitution of human hand with anthropomorphic structure, intuitive control and sensory feedback for dexterous motion restoration seems to come closer into our lives. Representative designs include the Smart hand, UB hand III, and Pisa/IIT hand in the laboratory condition, as well as the iLimb hand, Bebionic hand, and Vincent hand in the commercial. All of these designs focus on partial anthropomorphic characteristics, such as palm configurations, finger structures or actuation compliance; however, an ideal implementation of an anthropomorphic hand still lacks sufficient design guides and imposes a big challenge in the robotic community. A vague and inconsistent concept about the prosthetic hand's anthropomorphism makes researchers design their mechanical hands from various angles (biomechanical characters, grasps, sensing ability, etc.), receiving a great variety of robot hands featured with different levels of rehabilitation functions. In [1], Carl DiSalvo et al. give definition of anthropomorphism as "the act of attributing humanlike qualities to non-human organisms or objects", from which the humanlike qualities contain not only the hand's biological body, but also its philosophy function (action, sensation, and perception). From a view of system engineering, a prosthetic hand should encompass all of human hand's traits so that it can be called completely anthropomorphic; however, based on the current technology and limited understandings of our neural systems; a compromise must be done to receive an appropriate design. Then, a comprehensive index about the anthropomorphic level of a prosthetic hand to a human hand becomes necessary to make further evaluation and comparison through different designs. Concentrated on the hand's physical and actuation properties, this paper tends to evaluate the robot hand's anthropomorphism in a synthetic framework with 12 quantified indexes (QPHAEIs). We try to answer: 1) how to set-up the quantified prosthetic hand anthropomorphism indexes, 2) how anthropomorphic a prosthetic hand is, 3) how many indexes should be promoted to bridge the gap between human hand and prosthetic hand, 4) which is the lowest anthropomorphic index, and 5) how to improve the relatively low QPHAEIs. We ought to propose these evaluation indexes systematically, and detail and quantify each index as objective as possible. We also intend to improve some corresponding indexes by evaluating the anthropomorphic performance of current advanced prosthetic hands.

Previous evaluation research on prosthetic hands [2-10] mainly comprises two strategies. One is the robotic evaluation method that mainly concentrates on its evaluation on the prosthetic hand's kinematic and mechanical characteristics. For example, for evaluating the motion capability of a robotic or prosthetic hand, Feix et al. proposes a metric that utilizes Gaussian Process-Latent Variable Models (GP-LVM) to describe the finger's workspaces in some low-dimensional manifolds [2]. Liarokapis et al. compares the workspaces of the finger phalanges with those of the finger base frames [3]. Belter et al. discusses numerous mechanical design parameters by referencing examples in the literature, including number of actuators, hand complexity, weight, and grasp force [4-5]. Biagiotti et al. makes a thorough comparison on the robot hands of that time and attempts to relate some key-points of designing a dexterous robot hand to the hand's kinematics properties, aesthetic appearance, and its sensory system and control strategies [6]. Besides, according to end users' requirements, researchers from Scuola Superiore Sant'Anna propose a design methodology and assessment criteria of prosthetic hands to be used by transradial amputees. They also give a prosthetic hand design flow chart, in which the hand's volume is also a design evaluation index [7].The other hand evaluation strategy is established based on users' feedback about their prosthetic hands after daily use or specific tasks. Peerdeman et al. suggests some functional requirements for improving the acceptance of the myoelectric forearm prostheses by surveying the EMG sensing, control and feedback [8]. Dalley et al. employs the Southampton Hand Assessment Procedure (SHAP) to evaluate the prosthetic hand performance, which is simple and objective [9]. Through an

This work is supported in part by the National Basic Research Program (973 Program) of China (Grant No. 2011CB013306) and National Natural Science Foundation of China (51205080).

Yuan Liu, Dapeng Yang, Li Jiang, Hong Liu is with State Key Laboratory of Robotics and System, Harbin Institute of Technology, Harbin, 150080, China (e-mail: hityuanliu@hit.edu.cn, yangdapeng@hit.edu.cn, jiangli01@hit.edu.cn, dlrhitlab@aliyun.com. Tel: +86 451-86402330-827, Fex: +86 451-86418306).

internet survey, Pylatiuk et al. finds the most two dissatisfied items, weight and grasp speed, of the current prosthetic hands for amputees [10].

Although these meaningful efforts help us understand the-state-of-art of the current prosthetic hands, few of them present a comprehensive of evaluation indexes for quantifying hand anthropomorphism. Not only to reveal the gap between the prosthetic hand and natural hand (as did in the previous quantification efforts), but also we also try to find ways to bridge the gap. We tend to provide an easy, straightforward quantification criterion about the prosthetic hand's anthropomorphism. As a lot of anthropomorphism design indexes should be considered in the period of prototype design, the considered order of design indexes tends to be very important. We establish a consideration priority order in prosthetic hand's anthropomorphic index design to provide the reference for prosthetic hand designers.

Based on this motivation, the paper presents a total of 12 quantified prosthetic hand anthropomorphism evaluation indexes (QPHAEIs), for assessing the world's most popular commercial prosthetic hands, including the iLimb (Touch Bionics; Livingston, United Kingdom), Bebionic (RSL Steeper; Leeds, United Kingdom), Vincent (Vincent Systems; Weingarten, Germany), Michelangelo (Otto Bock; Duderstadt, Germany) hand, SensorHand speed(Otto Bock; Duderstadt, Germany), as well as the hand prototypes developed in our laboratory, HIT4 and HIT5. Our work starts from collecting reliable statistics from the human hand, to establishing a completed frame of anthropomorphism indexes on the hand's physical and actuation properties, and then to quantifying these indexes and evaluating the commercial prosthetic hands, and finally to proposing consideration priority order in

TABLE I. QUANTIFIED PROSTHETIC HAND ANTHROPOMORPHISM EVALUATION INDEXES

Index	QPHAEI	Index	QPHAEI
1	Whole Configuration	7	Length Ratio
2	Size	8	Range of Motion
3	Weight	9	Rotation Axis
4	Grasp Speed	10	Coupling speed ratio
5	Grasp Force	11	DOF Configuration
6	Compliance	12	Grasp Gesture

TABLE II. HUMAN FINGER PHALANGE LENGTH RATIO

Digit	MCP-PIP/ PIP-Tip Ratio (95% CI)	MCP-PIP/ PIP-DIP Ratio (95% CI)	PIP-DIP/ DIP-Tip Ratio (95% CI)
Index	1.02(0.006)	1.86(0.018)	1.24(0.018)
Middle	0.99(0.004)	1.72(0.013)	1.36(0.016)
Ring	0.95(0.007)	1.70(0.016)	1.29(0.016)
Pinky	0.98(0.007)	1.91(0.022)	1.06(0.022)

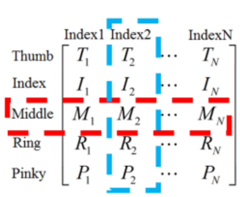

Figure 1 Evaluation parameter matrix

prosthetic hand's anthropomorphic index design.

This paper is organized as follows: Section II details the anthropomorphism evaluation framework with 12 QPHAEIs; Section III surveys the statistics of the 12 evaluation indexes for 11 kinds of prosthetic hands; Section IV presents the evaluation results and performs a correlation analysis on the evaluation results (7 most advanced commercial prosthetic hands in their product family); Section V presents a further analysis on the evaluation results; Section VI concludes the paper.

II. ANTHROPOMORPHISM EVALUATION METHOD

Based on the human hand's anatomy, literature review, end users' requirement, the 12 QPHAEIs is proposed in Table I. We put them into two categories as physical properties and actuation properties. As the difference of individual and finger motion, we have to choose the average as anthropomorphic criterion of prosthetic hand.

A. Evaluation of physical properties

The physical properties include the hand's *size*, *weight*, *finger phalange length ratio*, and *whole configuration*.

1) Size and weight evaluation:

By measuring the size of human hand, a reasonable length of the prosthetic hand should be in 180~198mm, while the width should be in 75~ 90mm [5][11]. The average weight of human hand is about 400g [12]. There is a common idea that when the size of a prosthetic hand exceeds its biological template, it will arouse much more attentions from the other people that decrease its anthropomorphism.

To quantify the hand's size index, the length and width were separately evaluated. Since the hand's length, including the fingers, is associated with fingertip trajectory and reachable workspace, while the hand's width is only associated with the mechatronics integrated space and aesthetic effect, we consider the hand length index is a slightly more important than hand width index and thus set the influence factors on the size index of the hand length and width as 60% and 40%, respectively.

Prosthetic hand length evaluation (M_L=(198+180)/2):

$$ES_L=\begin{cases}60\% & |\mathrm{L}-\mathrm{M}_L|\in[0,9]\\ \{1-[|\mathrm{L}-\mathrm{M}_L|-9]\times 0.02\}\times 60\% & |\mathrm{L}-\mathrm{M}_L|\in(9,19]\\ \{0.8-[|\mathrm{L}-\mathrm{M}_L|-19]\times 0.08\}\times 60\% & |\mathrm{L}-\mathrm{M}_L|\in(19,29]\\ 0 & |\mathrm{L}-\mathrm{M}_L|>29\end{cases} \quad (1)$$

Prosthetic hand width evaluation(M_W=(75+90)/2):

$$ES_W=\begin{cases}40\% & |W-M_W|\in[0,7.5]\\ \{1-[|W-M_W|-7.5]\times 0.04\}\times 40\% & |W-M_W|\in(7.5,12.5]\\ \{0.8-[|W-M_W|-12.5]\times 0.16\}\times 40\% & |W-M_W|\in(12.5,17.5]\\ 0 & |W-M_W|>17.5\end{cases}. \quad (2)$$

Prosthetic hand size evaluation:

$$ES=ES_L+ES_W\,. \quad (3)$$

Prosthetic hand weight evaluation:

$$EW = \begin{cases} 100\% & WE \in (0,400] \\ (1-\frac{WE\text{-}400}{300}) \times 100\% & WE \in (400,700] \\ 0 & WE \in (700,+\infty] \end{cases} . \qquad (4)$$

2) Finger phalange length ratio evaluation:

In Hamilton's study, the X-rays of 129 men and 68 women were examined. The ratio between the lengths of the finger phalanges are generalized in Table II [13]. Due to the strong diversity of the thumb, length ratios of the thumb's phalanges are not found in literature.

The length ratio of the finger phalanges is difficult to quantify since it contains numerous parameters largely dispersed. Therefore, the finger phalange length ratio has no overall quantification index. The whole configuration, DOF configuration, coupling speed ratio, range of motion, rotation axis direction and position and grasp gesture have similar problems. We introduce an evaluation matrix (human hand parameter matrix is M_H, prosthetic hand parameter matrix is M_R) to solve this problem, in which rows represents finger and columns represents evaluation indexes. The constructed form of evaluation parameter matrix is shown in Fig. 1.

If matrix A converges to matrix A' in the Euclid space, we can get:

$$\|A - A'\| \to 0$$

Matrix 2-norm is used to evaluate the convergence between the prosthetic hand parameter matrix (M_R) and human hand parameter matrix (M_H). In the following of this paper, subscript H indicates human hand, subscript R indicates prosthetic hand, and the text after the underline represents the name of the evaluation indexes (for example, LR in Equation 6 means the finger phalange's Length Ratio).

The evaluation algorithm is defined as

$$E = (1\text{-}\frac{\|M_R - M_H\|}{\|M_H\|}) \times 100\% . \qquad (5)$$

Based on Table II, finger phalange length ratio parameter matrix can be written as

$$M_{H\_LR} = \begin{bmatrix} 1.02 & 1.86 & 1.24 \\ 0.99 & 1.72 & 1.36 \\ 0.95 & 1.70 & 1.29 \\ 0.98 & 1.91 & 1.06 \end{bmatrix} . \qquad (6)$$

3) The whole configuration evaluation:

Hand anatomy study shows that each finger of the human hand has three bones with a large range of motion. The prosthetic hand's thumb should contain metacarpal, proximal phalange and distal phalange, while the four digits should have proximal phalange, intermediate phalange and distal phalange. The rows of the matrix mean the fingers (Fig. 1), while the columns of the matrix mean different phalanges. If there is a phalange in the corresponding matrix element location, the element is set to 1; otherwise the element is set to 0.

Therefore, the human hand whole structure parameter matrix is defined as： $M_{H\_WC} = Ones(5,3)$. (7)

B. Evaluation of actuation properties

Actuation properties of the hand include grasp speed, grasp force and functional grasp, compliance, range of joint motion, joint rotation axis direction and position, joint coupling speed ratio, DOF configuration and grasp gesture.

1) Grasp speed evaluation

Average finger velocities of MCP in the human's ADLs grasp are between 172°/s and 200°/s [14]. Since current prosthetic hands' motion is still slower than a natural hand, we take 172 °/s as the basic grasp speed criterion.

Prosthetic hand grasp speed evaluation is defined as follows:

$$E_{H\_S} = \begin{cases} 100\% & w_R \ge 172 \\ w_R / 172 & w_R < 172 \end{cases} . \qquad (8)$$

2) Grasp Force evaluation:

A study indicates that adult males could produce maximum forces of 95.6N for precision grasp, 103N for lateral grasp, and 400N for power grasp [15]. The percentage of time using in precision grasp, power grasp and lateral grasp was 20.9%, 46.5% and 12.0%, respectively, as shown in the Zheng's investigation on the grasp type and frequency [16]. We discussed the force evaluation within in these three main grasp functions. The functional gesture evaluation (detailed later), which intends to examine the hand's ability to accomplish different functional grasp, is measured by checking if the gesture-related objects in Cutkosky's grasp taxonomy [16] can be successfully picked by the prosthetic hand (achievable grasps). Percentages of the achievable functional grasp time in Cutkosky grasp taxonomy are $P_{Functional\_Precision}$, $P_{Functional\_Power}$ and $P_{Functional\_Lateral}$ respectively. Therefore, the grasp force and

TABLE III. COUPLING SPEED RATIO OF HUMAN HAND

Finger	PIP-MCP Ratio	DIP-PIP Ratio
Index	0.26	0.32
Middle	0.37	0.36
Ring	0.72	0.16
Pinky	0.70	0.25

TABLE IV. ACTIVE RANGE OF MOTION OF THE HUMAN HAND

Joint(Digit)	Flexion(°)	Extension(°)	Abduction/ Adduction(°)
MCP(Fingers)	About 90	30~40	About 30
PIP(Fingers)	>90	0	About 30
DIP(Fingers)	<90	0	0
CMC(Thumb)	17 ± 9		22 ± 9
MCP(Thumb)	60~70	50~60	19 ± 8.8
DIP(Thumb)	75~80	5~10	0

TABLE V. MCP PASSIVE ROTATION [27]

Digit's MCP	Rotation	Mean(SD) °
Index	Supination	15(7)
	Pronation	13(5)
Middle	Supination	14(6)
	Pronation	12(5)
Ring	Supination	20(7)
	Pronation	12(6)
Pinky	Supination	19(8)
	Pronation	14(6)

functional gesture evaluation can be calculated as: (P_W=20.9+46.5+12.0):

$$E_F = E_{F\_Precision} + E_{F\_Power} + E_{F\_Lateral} \tag{9}$$

$$E_{F\_Precision} \begin{cases} 1 \times \dfrac{P_{\text{Functional\_Precision}}}{P_W} \times 100\% & F_{Precision} \in [95.6, +\infty) \\ \dfrac{F_{Precision}}{95.6} \times \dfrac{P_{\text{Functional\_Precision}}}{P_W} \times 100\% & F_{Precision} \in [0, 95.6] \end{cases} \tag{10}$$

$$E_{F\_Power} \begin{cases} 1 \times \dfrac{P_{\text{Functional\_Power}}}{P_W} \times 100\% & F_{Power} \in [400, +\infty) \\ \dfrac{F_{Power}}{400} \times \dfrac{P_{\text{Functional\_Power}}}{P_W} \times 100\% & F_{Power} \in [0, 400] \end{cases} \tag{11}$$

$$E_{F\_Lateral} \begin{cases} 1 \times \dfrac{P_{\text{Functional\_Lateral}}}{P_W} \times 100\% & F_{Lateral} \in [103, +\infty) \\ \dfrac{F_{Lateral}}{103} \times \dfrac{P_{\text{Functional\_Lateral}}}{P_W} \times 100\% & F_{Lateral} \in [0, 103] \end{cases} . \tag{12}$$

TABLE VI. ROTATION AXIS POSITION AND DIRECTION EVALUATION INDEXES [17-26]

Finger	Joint	Evaluation index
Thumb	CMC /MCP	There are extension-flexion and abduction-adduction rotation axis (this has been evaluated in the DOF configuration evaluation, so this wasn't evaluated here)
		Extension-flexion rotation axis is in distal of abduction-adduction distal axis of rotation.
		Extension-flexion rotation axis direction trend is similar to Fig.2.
		Abduction-adduction rotation axis direction trend is similar to Fig.2.
	Opposition	In the thumb opposition grasp, thumb can produce cone movement.
	DIP	Extension-flexion rotation axis direction trend is similar to Fig.2.
Fingers	MCP	There are extension-flexion and abduction-adduction rotation axis (this has been evaluated in the DOF configuration evaluation, so this wasn't evaluated here)
		It is 60 degrees between abduction-adduction rotation axis and the corresponding metacarpal.
		Extension-flexion rotation axis direction trend is similar to Fig.2. The incline trend gradually increases from index finger to pinky. Index finger inclination angle is negative，middle finger and pinky inclination angle are positive.
	PIP/DIP	Extension-flexion rotation axis direction trend is similar to Fig.2. Index finger can be seen as no incline. The incline trend gradually increases from middle finger to pinky.

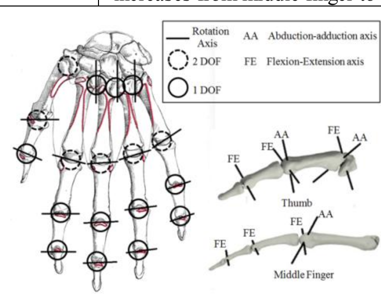

Figure 2 Human hand rotation axis configuration

3) DOF configuration evaluation:

An accurate hand kinematic model is necessary for evaluating the prosthetic hand's degrees of freedom (DOF) configuration. After a thorough comparison of the kinematic models proposed in the literature [17-25], inspired by Ian M. Bullock's critical review [25] we finally utilized the Anne Hollister's the thumb kinematic model [17-18] and Georg Stillfried's palm and finger kinematic model [19] as our DOF configuration evaluation criterion. Thus, in our DOF configuration evaluation, the thumb contains five DOFs (each of CMC and MCP has two, DIP has one); each finger contains four DOFs (MCP has two, each of PIP and DIP has one). Palm contains three DOFs. There is one DOF (abduction) between each two adjacent metacarpal of four fingers.

In the index matrix of DOF configuration, if there is an artificial DOF in corresponding position, the element of the matrix is set to 1, otherwise 0. In Georg Stillfried's kinematic model, three rotational axes of palm are all along the axis of the forearm. The palm's motion, realized by carpometacarpal (CMC) joint synergy motion of abduction-adduction and flexion-extension, is mainly accomplished by the metacarpals of index finger, ring finger and pinky. Therefore, we split the palm's DOF parameter into these three fingers in the index matrix as their abduction-adduction and flexion-extension of the CMC joint is 0.5. These first two elements of the parameter vector of the middle finger (the third row in M_{H_DOF}) are set to 0. The overall index matrix of the DOF configuration is shown in Equation 13 (matrix column from 1st to 6th were CMC extension-flexion, CMC abduction-adduction, MCP extension-flexion, MCP abduction-adduction, PIP extension-flexion, DIP extension-flexion, respectively).

$$M_{H\_DOF} = \begin{bmatrix} 1 & 1 & 1 & 1 & 0 & 1 \\ 0.5 & 0.5 & 1 & 1 & 1 & 1 \\ 0 & 0 & 1 & 1 & 1 & 1 \\ 0.5 & 0.5 & 1 & 1 & 1 & 1 \\ 0.5 & 0.5 & 1 & 1 & 1 & 1 \end{bmatrix} \tag{13}$$

4) Coupling speed ratio evaluation:

According to Fig.1 and human hand coupling speed ratio (Table III), human hand coupling speed ratio parameter matrix can be written as

$$M_{H\_CR} = \begin{bmatrix} 0.26 & 0.32 \\ 0.37 & 0.36 \\ 0.72 & 0.16 \\ 0.70 & 0.25 \end{bmatrix} . \tag{14}$$

5) Range of motion evaluation:

Kapandji details the range of motion of human hand joint, as shown in Table IV [26]. In order to calculate and quantify accurately, the active motion range of finger joint is normalized by using Equation (15). Index j from 1-7 indicates the CMC rotation, MCP extension, MCP flexion, MCP abduction-adduction, PIP flexion, DIP flexion, and DIP extension.

$$R_{ij} = \frac{Range_R}{Range_H} \times 100\% \tag{15}$$

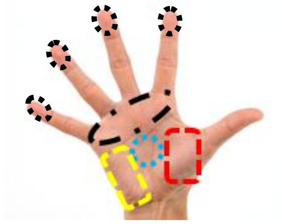

Figure 3 Finger pad and palm compliance configuration

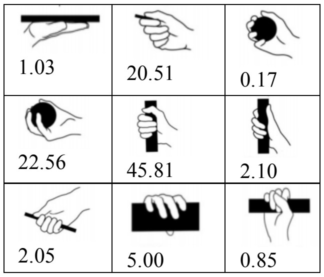

Figure 4 Power grasp parameter matrix

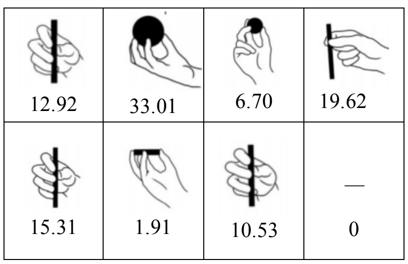

Figure 5 Precision grasp parameter matrix

Then, the parameter matrix of the active range of motion of a human hand is:

$$M_{H\_AR} = Ones(2,7) \tag{16}$$

6) Compliance evaluation:

Passive DOF's of a human hand joint in the literature contain both passive rotation (Table V) [27] and passive extension of MCP and DIP. Human hand MCP passive extension can achieve 60 degrees, while finger DIP passive extension can achieve 30 degrees [26].

According to Fig.1, the human hand compliance parameter matrix is made up of passive extension of MCP and DIP, passive rotation of MCP and the soft pad (1 represents soft contact deformation, 0 means no compliance there). We constructed the index matrix of the hand compliance as a 4×6 matrix, with the columns of the upper-left 4×4 submatrix representing the MCP Supination, MCP Pronation, MCP passive extension, and DIP passive extension in turn, and the rows representing the index finger to the pinky, respectively. The fifth column represents the finger fingertip pad adaptive deformation, and the sixth column represents the palm adaptive deformation (as shown in Fig. 3). The first element to the fourth element in the sixth column represent adaptive deformation of thenar, hypothenar, root of finger and palmar.

Due to the different units adopted in the matrix, the former 4 columns were normalized. These former 4 columns of the prosthetic hand parameter matrix were calculated by using a method similar to Equation (15). Each element of prosthetic hand parameter matrix was calculated according to Equation (15), with all parameters in human hand parameter matrix setting to 1. Because passive movement within the thumb is still unclear in the literature, we only evaluated the finger compliance without thumb. Human hand compliance matrix can be written as

$$M_{H\_PR} = Ones(4,6)\,. \tag{17}$$

7) Rotation axis evaluation:

Due to the prosthetic hand's limited weight, volume and current technology, currently there is no prosthetic hand that can fully realize the kinematic of a human hand. The ACT gets closer to a real human-hand kinematic; however, it also needs to do some simplification in the finger joints [28]. Therefore, we made general design requirements about the kinematics model, as shown in Table VI. Specifically, we do not consider the DOF configuration (evaluated in another index) in the joint axis's direction and position evaluation, because we find that even a prosthetic hand, such as the Michelangelo hand, has a small number of DOFs, it may still have a high index of the rotation axis evaluation. We put each index of the Table VI in a 21-dimensional vector, with satisfied elements setting to 1 (otherwise 0). The index matrix (joint rotation axis position and direction matrix) of the human hand can be written as

$$M_{H\_AOP} = Ones(1,21)\,. \tag{18}$$

We adopt Equation (5) to evaluate the index matrix of this anthropomorphic character.

8) Grasp gesture evaluation:

Based on Zheng's research [16], the power grasp, precision grasp and no grasp percentage of time are 42.4%, 15.1% and 42.5%. The human hand's PIP and MCP joints in no-grasp state (also termed as neutral mode) have a large flexion, while DIP joints only flex little.

We constituted two parameter matrixes separately for the human hand power grasp (Fig.4) and precision grasp (Fig.5). The prosthetic hand parameter matrix's elements were all obtained by multiplying 1 (achievable) or 0 (unachievable) to the elements with the human hand's parameter power grasp matrix and precision grasp parameter matrix.

The quantitative evaluation of grasp gesture equation can be written as (E_{G_Power} , $E_{G\_Precision}$, $E_{G\_Neutral}$ in Equation 19 are calculated according to Equation 5):

$$E_G = E_{G\_Power} \times 42.4\% + E_{G\_Precision} \times 15.1\% + E_{G\_Neutral} \times 42.5\%\,. \tag{19}$$

At last, we define the global anthropomorphic score (GAS) of a prosthetic hand as the summation of the weighted 12 index factors:

$$E_{Global} = ES \times w_S + EW \times w_W + E_{WC} \times w_{WC} + E_{LR} \times w_{LR} + E_S \times w_{GS} + E_F \times w_F + E_{DOF} \times w_{DOF} + E_{CR} \times w_{CR} + E_{AR} \times w_{AR} + E_{PR} \times w_{PR} + E_{AOP} \times w_{AOP} + E_G \times w_G\,. \tag{20}$$

Where w_* are the weighted factors that evenly equal 1/12. We consider each of the anthropomorphic indexes equally influential. Note that these weighs can be changed according to specific evaluation target. For example, for evaluation of a dexterous hand, the coefficients of weight or size can be reduced.

III. PROSTHETIC HAND STATISTIC

Mainly based on Belter's study [4-5], we made an updated survey about the prosthetic hands with new Bebionic 3 and iLimb ultra revolution being introduced. Compared with Bebionic 2, Bebionic 3 weighs a little heavier (550-598g) and its grasp force becomes larger (power, tripod and lateral grasp force is 140.1N, 36.6N and 26.5N) [29]. Compared with iLimb ultra, iLimb ultra revolution weighs 443-451g (without wrist) and has an additional active thumb opposition DOF [30]. Parameter of the prosthetic hands, HIT4 and HIT5, were collected from [31][32].

IV. ANTHROPOMORPHISM EVALUATION RESULT

In specific, four multifunctional prosthetic hands in the commercial, the iLimb ultra revolution, Bebionic 3, SensorHand speed and Michelangelo hand, are within my research scope since they are the representative hands in practice and have a large portion of users around the global. Since Vincent Hand has a lot of missing data, Vincent Hand is utilized in some circumstances. Two commercial candidates, HIT 4 and HIT 5, from our laboratory are also included in the research for some comparative analysis, as well as in the correlation analysis of the design specifications.

A. Twelve QPHAEIs Evaluation Results of 6 Commercial Prosthetic Hands

Fig. 6 shows the evaluation results (distribution trends) of the 12 QPHAEIs and GAS of the 6 advanced prosthetic hands (iLimb ultra revolution is replaced by the iLimb in the figure).

B. Mean evaluation values of 12 QPHAEIs

Fig.7 shows the mean evaluation values of 12 QPHAEIs on four most advanced commercial prosthetic hands (Bebionic 3, Michelangelo hand, ilimb-ultra revolution and SensorHand speed). The value up each bar is the mean value of corresponding QPHAEI. Error bar shows the maximum and

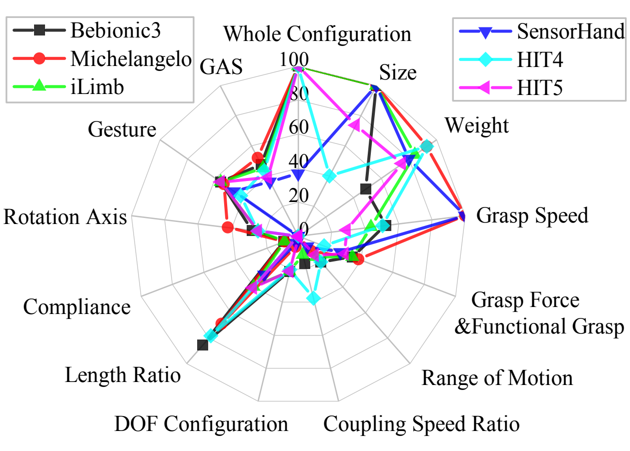

Figure 6 Twelve QPHAEIs Evaluation Results Distribution Trends of 6 Commercial Prosthetic Hands

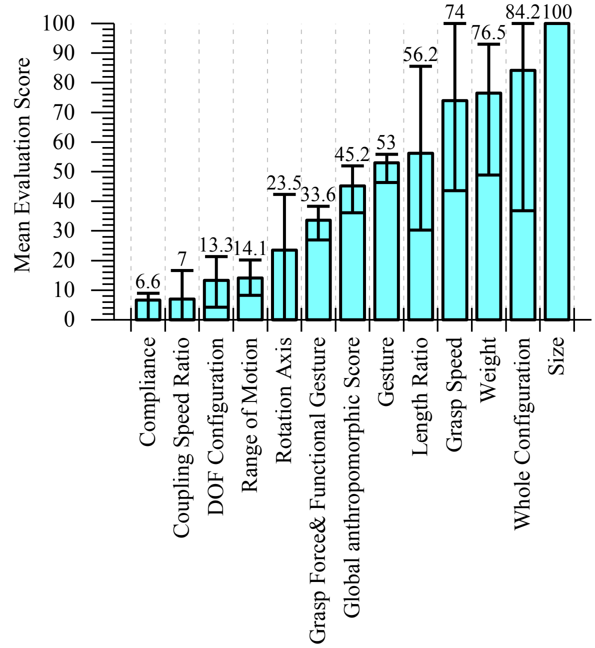

Figure 7 Mean Evaluation Result Comparison Figure of 12 QPHAEIs

minimum value in each QPHAEI.

C. Twelve QPHAEIs Correlation analysis

As a lot of design indexes should be considered in the period of prototype design, the considered order of design indexes tends to be very important. A consideration priority order in prosthetic hand's anthropomorphic index design is established by using correlation analysis method. The relationship between the 12 indexes and the GAS is analyzed by using correlation analysis method. A correlation matrix is built including all of the 12 evaluation indexes and the final GAS across all six prosthetic hands (iLimb ultra revolution, Bebionic 3, Michelangelo hand, SensorHand speed, HIT4 and HIT5). The absolute values of corresponding correlation coefficients are averaged across all six prosthetic hands. The stronger the correlation is, the greater the impacts on other indexes are, and higher consideration priority the corresponding anthropomorphic design index should be had. The consideration priority in prosthetic hand's anthropomorphic index design and correlations between QPHAEIs and GAS are shown in Fig.8.

V. DISCUSSION

The global anthropomorphic score (GAS) of the current 4 most advanced prosthetic hand (iLimb ultra revolution, Bebionic 3, SensorHand speed and Michelangelo hand) can only achieve 45.2%, as shown in Fig.6. The Michelangelo hand is the only hand with GAS more than a half (51.9%). From Fig.5, it is clear that the high anthropomorphism indexes are all from the category of physical properties

It can be seen from Fig.6 and Fig.7 that current commercial prosthetic hand's size and whole configuration nearly reach their anthropomorphism design request. It is surprising that the

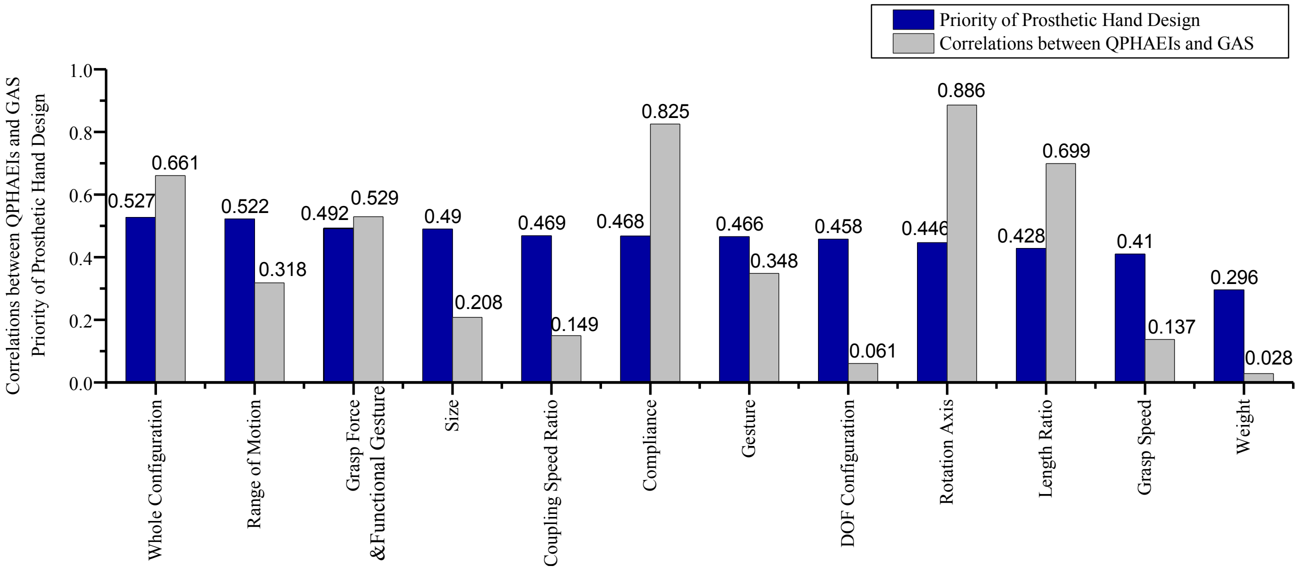

Figure 8 Prosthetic hand design priority and correlations between QPHAEIs and GAS

phalange length ratio, which is an easy design, only reaches 56.2%. It also shows that the Bebionic3 has the most anthropomorphic appearance. Its whole configuration, size and phalange length ratio rank the first. Evaluation results on grasp gesture show that the individually driven commercial prosthetic hands (iLimb ultra revolution, Bebionic3, Vincent hand, HIT5) have comparatively high performance. For gesture, current commercial prosthetic hands only reach 53% of that of a human hand. Prosthetic hands having 5 individually driven fingers and a rotation thumb can achieve 96.2% of power grasp, and only Disk (power grasp parameter matrix (1,3)), Adducted Thumb (power grasp parameter matrix (2,3)), Light Tool (power grasp parameter matrix (3,1)) in Cutkosky grasp taxonomy cannot be completed. Both Michelangelo hand's and SensorHand speed's PIP and DIP have fixed angles, behaving like a human hand like in a relaxed posture (neutral mode). It will produce a high anthropomorphism appearance. Since the neutral mode accounts for about 42.43% of in the housework [16], it is essential to the gesture evaluation. The average evaluation result of the rotation axis position and direction of current commercial prosthetic hands is only 23.5%. The thumb rotation axis receives the worst anthropomorphism. All of the current commercial prosthetic hands do not have a proper rotation axis distribution on the thumb. Michelangelo hand has the highest index value in rotation axis position and direction evaluation (hand kinematics configuration). The average active range of the commercial prosthetic hand motion is only 14.1%.

The DOF configuration, coupling ratio and compliance are the lowest QPHAEIs. Evaluation result on the DOF configuration of current commercial prosthetic hands is 13.3%. It may be attributed to two main reasons: few dependent DOFs and non-anthropomorphic DOF configuration. The evaluation result on coupling ratio is 7%. Although our results on coupling ratio is rough, it is still applicable. A human-like finger trajectory is important to grasp objects. Finger trajectory is determined by phalange length ratio and coupling speed ratio, while the coupling speed ratio is highly related to human hand's joint angles in different grasp tasks. Since only a few of motors can be integrated in an intrinsically-driven prosthetic hand, we do have to reduce the dimensions of the controllable joint variables. This can be done by using a synergic actuation through direct coupling or underactuation mechanisms. In the future, we will take the reproduced fingertip trajectory as the anthropomorphism evaluation index of the coupling speed ratio to evaluate and design new prosthetic hands.

For the compliance, current commercial prosthetic hands only have fingertip pad and palm adaptive deformation. Vincent hand compliance performance performs the best in all 7 prosthetic hands. The newly developed cosmetics glove consists of pigmented high temperature silicon with reinforcement in the finger pads and the inside of the hand. This glove is made of silicon foam to imitate the formation of folds and improves the adaptation characteristics. In the future, we will measure the human hand's compliance performance in different gestures. The measured data will then become a basis of research prosthetic hand evaluation.

The correlation analysis between 12 QPHAEIs and the GAS can be seen in Fig 8. It can be seen that the mean correlation coefficients between all 12 QPHAEIs are relatively low, which verifies the irredundant of the QPHAEIs. Stronger correlation means greater impact of the QPHAEI on the others, which needs a higher design consideration priority. It is clear that the whole configuration, range of motion, grasp force and functional grasp should be considered firstly in a prosthetic hand design. From this correlation analysis between QPHAEIs and GAS, the anthropomorphism index of rotation axis distribution had a highest correlation coefficient (0.886) with the GAS, while the anthropomorphism index of the gesture has a low correlation coefficient (0.348) with the GAS. It indicates that the rotation axis distribution, rather than experimental grasp gesture, is reliable index to evaluate the prosthetic hand's GAS.

VI. CONCLUSION

In this paper, we presented an evaluation framework on prosthetic hands' anthropomorphism with 12 QPHAEIs. The corresponding QPHAEIs of human hand were collected from the literature. They can be directly served as the design criterion. We applied our quantifying anthropomorphism evaluation method on 7 most-popular prosthetic hands and obtained a preliminary result on the hands' performance. Through the correlation analysis of the hands' 12 QPHAEIs, consideration priority order in prosthetic hand's anthropomorphic index design was also received. This evaluation framework is simple and can be applied in any anthropomorphic robot hand. In the future, we will concentrate on the coupling speed ratio and compliance evaluation. The EMG control algorithm also will be evaluated in a virtual reality environment. System engineering modeling and validation methods will also be used. Based on these evaluation methods, we hope to provide more systemic and scientific strategy for designing dexterous prosthetic hands.

ACKNOWLEDGMENT

This work was partly supported by the National Basic Research Program (973 Program) of China (Grant No. 2011CB013306) and National Natural Science Foundation of China (51205080).

REFERENCES

[1] C. DiSalvo and F. Gemperle, "From seduction to fulfillment: the use of anthropomorphic form in design," in Proceedings of the 2003 international conference on Designing pleasurable products and interfaces, 2003, pp. 67-72.

[2] T. Feix, J. Romero, C. H. Ek, H. B. Schmiedmayer, and D. Kragic, "A Metric for Comparing the Anthropomorphic Motion Capability of Artificial Hands," Ieee Transactions on Robotics, vol. 29, pp. 82-93, Feb 2013.

[3] M. V. Liarokapis, P. K. Artemiadis, and K. J. Kyriakopoulos, "Quantifying Anthropomorphism of Robot Hands," 2013 Ieee International Conference on Robotics and Automation (Icra), pp. 2041-2046, 2013.

[4] J. T. Belter and A. M. Dollar, "Performance characteristics of anthropomorphic prosthetic hands," IEEE Int Conf Rehabil Robot, vol. 2011, p. 5975476, 2011.

[5] J. T. Belter, J. L. Segil, A. M. Dollar, and R. F. Weir, "Mechanical design and performance specifications of anthropomorphic prosthetic hands: a review," J Rehabil Res Dev, vol. 50, pp. 599-618, 2013.

[6] L. Biagiotti, F. Lotti, C. Melchiorri, and G. Vassura, "How far is the human hand," A review on anthropomorphic robotic end-effectors, 2004.

[7] C. Cipriani, M. Controzzi, and M. C. Carrozza, "Objectives, criteria and methods for the design of the SmartHand transradial prosthesis," Robotica, vol. 28, pp. 919-927, Oct 2010.

[8] B. Peerdeman, D. Boere, H. Witteveen, R. H. in 't Veld, H. Hermens, S. Stramigioli, et al., "Myoelectric forearm prostheses: state of the art from a user-centered perspective," J Rehabil Res Dev, vol. 48, pp. 719-37, 2011.

[9] S. A. Dalley, D. A. Bennett, and M. Goldfarb, "Preliminary functional assessment of a multigrasp myoelectric prosthesis," Conf Proc IEEE Eng Med Biol Soc, vol. 2012, pp. 4172-5, 2012.

[10] C. Pylatiuk, S. Schulz, and L. Doderlein, "Results of an Internet survey of myoelectric prosthetic hand users," Prosthet Orthot Int, vol. 31, pp. 362-70, Dec 2007.

[11] Touch Bionics web site [Internet]. Mansfield (MA): Touch Bionics Inc; 2013. Available from: http://www.touchbionics.com/

[12] R. Chandler, C. Clauser, J. McConville, H. Reynolds, and J. Young, "Investigation of inertial properties of the human body," DTIC Document1975.

[13] R. Hamilton and R. Dunsmuir, "Radiographic assessment of the relative lengths of the bones of the fingers of the human hand," Journal of Hand Surgery (British and European Volume), vol. 27, pp. 546-548, 2002.

[14] J. H. Bowker, J. W. Michael, and A. A. o. O. Surgeons, Atlas of limb prosthetics: surgical, prosthetic, and rehabilitation principles: Mosby Year Book, 1992.

[15] C. L. Taylor, "Control design and prosthetic adaptations to biceps and pectoral cineplasty," Human Limbs and Their Substitutes. New York, McGraw-Hill International Book Co, 1954.

[16] J. Z. Zheng, S. De La Rosa, and A. M. Dollar, "An Investigation of Grasp Type and Frequency in Daily Household and Machine Shop Tasks," 2011 Ieee International Conference on Robotics and Automation (Icra), 2011.

[17] A. Hollister, W. L. Buford, L. M. Myers, D. J. Giurintano, and A. Novick, "The axes of rotation of the thumb carpometacarpal joint," Journal of Orthopaedic Research, vol. 10, pp. 454-460, 1992.

[18] A. Hollister, D. J. Giurintano, W. L. Buford, L. M. Myers, and A. Novick, "The axes of rotation of the thumb interphalangeal and metacarpophalangeal joints," Clinical orthopaedics and related research, vol. 320, pp. 188-193, 1995.

[19] G. Stillfried and P. van der Smagt, "Movement model of a human hand based on magnetic resonance imaging (MRI)," in International Conference on Applied Bionics and Biomechanics (ICABB), 2010.

[20] F. P. van der Hulst, S. Schatzle, C. Preusche, and A. Schiele, "A functional anatomy based kinematic human hand model with simple size adaptation," in Robotics and Automation (ICRA), 2012 IEEE International Conference on, 2012, pp. 5123-5129.

[21] J. Lenarčič, T. Bajd, and M. M. Stanišić, "Kinematic Model of the Human Hand," in Robot Mechanisms, ed: Springer, 2013, pp. 313-326.

[22] M. Tsai, H. Lee, and H.-C. Chen, "Construction of a Realistic Hand Model with 22 Joint Freedoms," in 13th World Congress in Mechanism and Machine Science, 2011.

[23] P. Cerveri, E. De Momi, N. Lopomo, G. Baud-Bovy, R. Barros, and G. Ferrigno, "Finger kinematic modeling and real-time hand motion estimation," Annals of biomedical engineering, vol. 35, pp. 1989-2002, 2007.

[24] L. Y. Chang and N. S. Pollard, "Method for determining kinematic parameters of the in vivo thumb carpometacarpal joint," Biomedical Engineering, IEEE Transactions on, vol. 55, pp. 1897-1906, 2008.

[25] I. M. Bullock, J. Borràs, and A. M. Dollar, "Assessing assumptions in kinematic hand models: a review," in Biomedical Robotics and Biomechatronics (BioRob), 2012 4th IEEE RAS & EMBS International Conference on, 2012, pp. 139-146.

[26] I. A. Kapandji, The physiology of the joints, 2nd ed. New York: Churchill Livingstone, 1982.

[27] J. Krishnan and L. Chipchase, "Passive axial rotation of the metacarpophalangeal joint," The Journal of Hand Surgery: British & European Volume, vol. 22, pp. 270-273, 1997.

[28] A. D. Deshpande, Z. Xu, M. V. Weghe, B. H. Brown, J. Ko, L. Y. Chang, et al., "Mechanisms of the anatomically correct testbed hand," Mechatronics, IEEE/ASME Transactions on, vol. 18, pp. 238-250, 2013.

[29] Bebionic3 Product Brochure. Leeds(United Kingdom): RSL Steeper;2012.

[30] i-limb ultra revolution datasheet. Livingston(United Kingdom): Touch Bionics;2013.

[31] H. Liu, D. Yang, L. Jiang, and S. Fan, "Development of a multi-DOF prosthetic hand with intrinsic actuation, intuitive control and sensory feedback " Industrial Robot: An International Journal, vol. 41, pp. 381-392, 2014.

[32] L. Jiang, B. Zeng, S. Fan, K. Sun, T. Zhang and H. Liu, "A Modular Multisensory Prosthetic Hand," in Proceeding of the IEEE International Conference on Information and Automation, 2014, pp.648-653.